LASER ULTRASONIC AND PHOTOACOUSTIC CHARACTERIZATION OF SUBSURFACE STRUCTURES

Meng-Chou Wu
Department of Physics
College of William and Mary
Williamsburg, VA 23185

F. Raymond Parker and William P. Winfree
NASA, Langley Research Center
MS 231
Hampton, VA 23681

INTRODUCTION

There is a strong interest in applying laser ultrasonic and photoacoustic techniques to the NDE of some high performance structures, for example, the actively cooled panels of the National Aero-Space Plane. Both laser ultrasonic and photoacoustic techniques have been developed for years. Much significant work has been done on either the generation of waves, the mechanisms [1-3] or various techniques for the detection of these waves [4-6]. A few applications being pursued or conducted since the early stage of the development for these techniques [5-7]. However, there is little work concentrating on the interaction of these waves with structures and materials [8]. For successfully applying the laser ultrasonic and photoacoustic techniques to the NDE of a practical system, it is important to understand the interaction of laser generated ultrasounds and thermal waves with, for example, the subsurface structures or defects in the materials and their relationship to images obtained from the techniques.

There are two focuses for this research. One is a comparison of laser ultrasonic and photoacoustic imaging; the other is the application of these techniques to the characterization of subsurface structures and defects.

GENERATION OF WAVES

When an intensity-modulated or Q-switched laser beam illuminates the surface of a solid, in general, a part of the electromagnetic energy is absorbed and a temperature field and an acoustic source are created due to the thermoelastic properties of the solid. The thermal waves are generated as the results of temperature variation and thermal energy propagation in the solid. The ultrasonic waves are generated by the thermoelastic stress of the heated area. The propagation of these two types of waves determines their different behaviors.

Review of Progress in Quantitative Nondestructive Evaluation, Vol. 12
Edited by D.O. Thompson and D.E. Chimenti, Plenum Press, New York, 1993

The thermal waves are damped with a thermal diffusion length μ.

$$\mu = (2\kappa/\omega)^{1/2}$$

where κ is the diffusivity and ω the angular frequency of the modulation. For aluminum, the thermal diffusion length μ is about 0.5mm at 100Hz and 5μm at 1MHz. For application of these techniques to investigate a typical sample with thickness of a few mm, apparently the thermal waves dominate at lower modulation frequencies, say below 1kHz, since the acoustic wavelength becomes too long to probe the sample. While the ultrasonic waves dominate when using a Q-switched laser beam as the frequency ranges of the waves are broader but well above hundreds of kHz and thermal waves penetrate only slightly below the surface. In other words, the two different types of waves are coupled in generation in general; however, can be separated for applications in practice. This results in the development of two types of techniques, laser ultrasonics and photoacoustics.

EXPERIMENTAL SETUP

In Fig. 1, the block diagram shows the experimental setup for the laser ultrasonic imaging. A Q-switched YAG laser beam was used to scan over the front surface of a sample. A piezoelectric (PZT) transducer was bonded to the back surface of the sample. The detected signals were fed through the digitizer and, for each step, digitized wave forms were recorded. The wave forms were stored in a computer for future analysis. A typical laser ultrasonic wave form from a steel sample is shown in Fig. 2. Usually the initial part of the wave form (about 1μs long) was used for imaging.

The application of the laser generated thermal waves to the photoacoustic imaging for this research is shown in Fig. 3. A CW YAG laser was used and the beam was chopped at a selected frequency. Similar to the laser ultrasonic technique, a piezoelectric transducer was used as a detector. It replaced the air-microphone ensemble used in traditional photoacoustic techniques. It detects thermal waves acoustically, therefore the technique is still photoacoustic. The signals were fed through a lock-in amplifier and both the magnitude and the phase were recorded as functions of positions. Although the entire wave form was not used for imaging in this case, a typical photoacoustic wave form of a steel sample is shown in Fig. 4 for comparison. (To get a wave form, the signal was directly fed through the digitizer without the lock-in amplifier.) The chopping frequency is 45Hz for this case. The wave form reflects the temperature variation, heating and cooling, detected by the transducer.

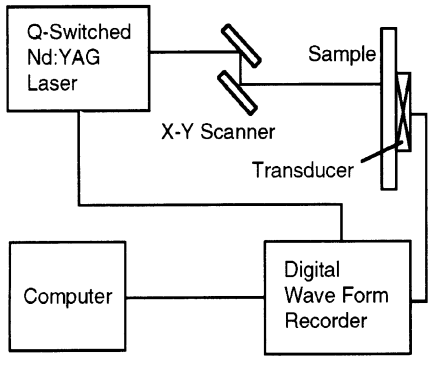

Fig. 1 Block diagram of laser ultrasonic imaging.

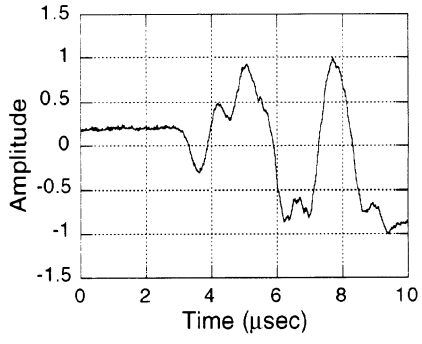

Fig. 2 A typical laser ultrasonic wave form of a steel sample.

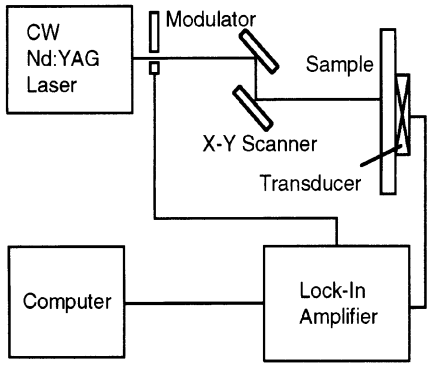

Fig. 3 Block diagram of photoacoustic imaging.

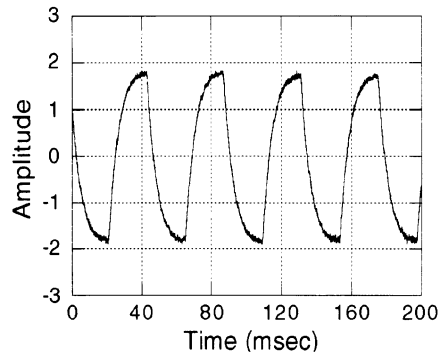

Fig. 4 A typical photoacoustic wave form detected by the piezoelectric transducer.

IMAGING

As the laser beam scanned over the sample surface, for each step, a digitized wave form from the laser ultrasonic signals was recorded. The amplitude of a wave form at a fixed time was used to represent a pixel (x_k, y_j) for an image of the scanned area as $A(x_k, y_j; t_i)$ with the consecutive points of the wave form representing the time evolution of the pixel. The whole wave forms at all positions therefore resulted a series of images similar to movie frames.

For the photoacoustic thermal wave imaging, both the magnitude A(x, y) and the phase $\phi(x, y)$, recorded as functions of positions were transformed into images. All the images are finally normalized to a 256-level gray or color scale, without any further processing, for presentation.

RESULTS AND DISCUSSION

Fig. 5 is a laser ultrasonic image of a piece of steel with a two-dimensional structure.

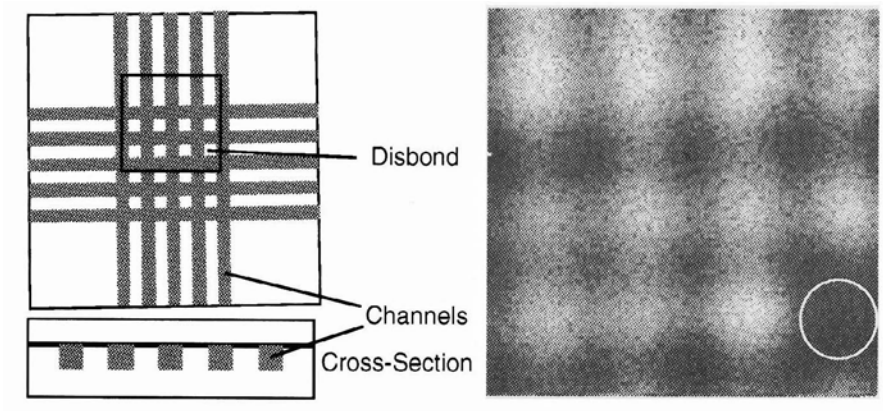

Fig. 5 The laser ultrasonic image of a steel sample with two-dimensional channels. The scan area is 7.5mm x 7.2mm. The missing bright spot indicates a disbond.

The sample has two plates with milled channels and diffusion-bonded together. The thickness of the sample is about 3.3mm and the width of the channels is 1mm. The image shows clearly a missing spot for a fabricated disbond.

For better understanding how laser ultrasonic images reveal the subsurface structures, measurements were done on an aluminum sample with one-dimensional channels. The sample is about 12mm by 12mm with a thickness of 3mm. Several cylindrical holes with 1mm diameter run through the sample and are nearly parallel to the square surface. Fig. 6(a) is the laser ultrasonic image of the sample. The channels are clearly shown. The image even reveals the three-dimensional characteristics of the cylindrical structure. However, the columns on the image assess larger than actual dimensions. There are certainly many factors contributing to that. The fundamental limitation of resolution related to the depth and the wave lengths is not going to be discussed here. What is considered is the effects of the laser beam sizes on the resulting images.

The beam size used for the image shown in Fig. 6(a) is about 1mm. The scan step size is much smaller, only 0.06mm. Fig. 6(b) shows another image of the same sample with a reduced beam size of about 0.05mm but the same scan step. (The laser power was reduced

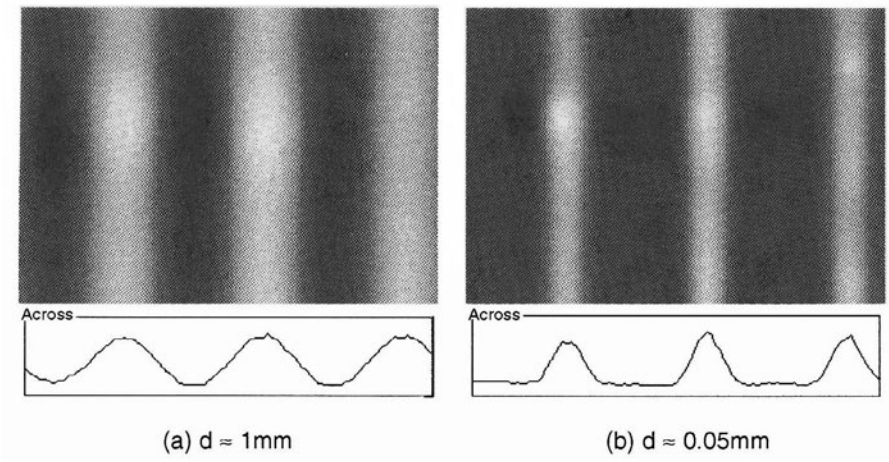

Fig. 6 The laser ultrasonic images of a aluminum sample with one-dimensional cylindrical channels. The channels have a diameter of about 1mm. The scan area is 6mm x 4.2mm The laser beam size is about 1mm for (a) and 0.05m for (b). Below the images are the amplitude profiles measured across the bottom scan line.

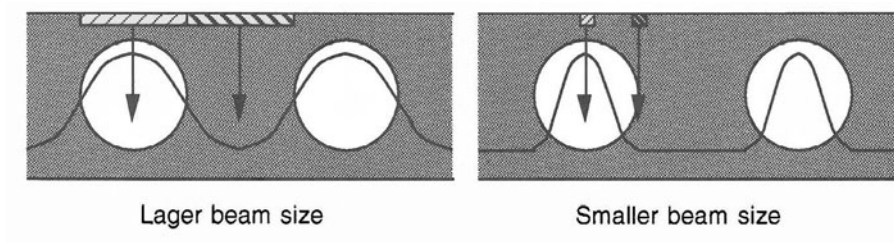

Fig. 7 The model of beam size effects on the laser ultrasonic images. The corresponding spot size and the way of wave propagation are simplified in this picture. The curves describes qualitatively the relative change of the amplitude for the detected signals.

for this case to keep the generation in thermoelastic regime.) The image gives the similar pattern for the structure, however, with different width. Fig. 7 illustrates schematically the situation for both cases. For a broader beam, as it scans over the area of the channels, there are some positions where the incident waves have only a portion diffracted by the structure. The curve in the picture describes qualitatively the relative change of the signal amplitude for the scan. By contrast, the smaller beam gives better defined boundaries. The amplitude profiles measured directly from two images of Fig. 6, shown below each, reflect the difference.

It is noticeable that both the images in Fig. 6(a) and Fig. 6(b) have a band across the image with higher contrast than the rest of the area. That is a result of a black mark drawn on the surface of the sample. The enhancement in the amplitudes of laser generated ultrasonic waves by surface treatments has been investigated by some researchers [2], and these images agree with their results.

It is of interest to see how surface treatments affect the generated thermal waves and thereby the resulted photoacoustic images. Fig. 8(a) shows the photoacoustic magnitude image of the same sample discussed previously. Similarly there is a black line on the surface. The contrast enhanced by the paint effect is much higher than that shown in the laser ultrasonic images. The relative change of the amplitudes resulted from the black paint is more than 40db as shown in the image. However, in the photoacoustic phase image, Fig. 8(b), the existence of the paint is not visible. In general the surface treatments have a significant effect on the magnitude images but not on the phase images. This is also clearly seen in an aluminum

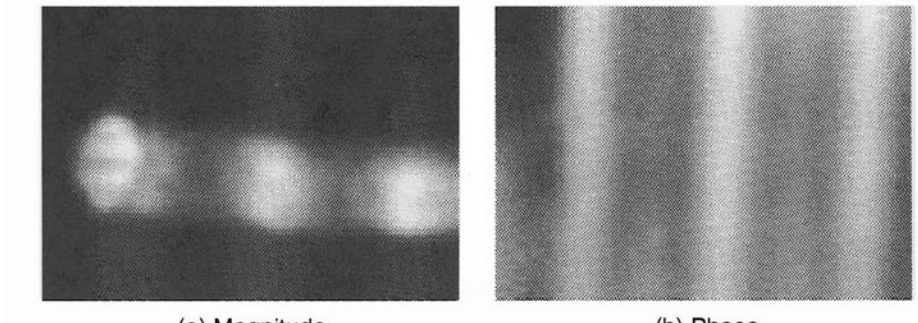

Fig. 8 The photoacoustic images of the same aluminum sample as shown in Fig.6. A black mark line was drawn from the left across the sample surface The magnitude image is enhanced by the line. The phase image almost ignore its existence.

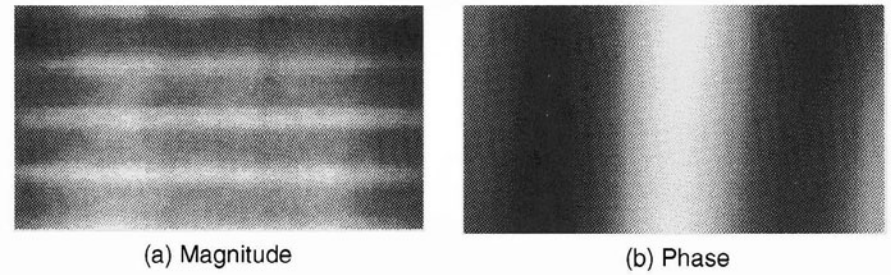

Fig. 9 The photoacoustic images of another aluminum sample with two channels, which have a diameter of 2mm. The scan area is 6.6mm x 3.6mm. Five horizontal lines shown in the magnitude image (a) are the scratches on the sample surface.

sample with surface scratches on it. The sample has two larger channels whose diameter is about 2mm. The very shallow surface scratches were created by a high power, confined laser beam. As shown in Fig. 9(a), the scratches have a strong effect on the magnitude image, and again, on the phase image shown in Fig. 9(b), their existence is not apparent.

Examination of the widths of the channels shown on the image of Fig. 8(b) indicate a change in the width along the channel. The channels in the sample actually have a small angle away from the surface. The different widths on the image reflect the different depths of the channel under the surface. The deeper the channel the narrower the width shown in the image. The phase images are more sensitive to the change of depths than the magnitude images are [7]. This feature allows a characterization of the depth for the structure from photoacoustic images.

The ultrasonic images can be used to characterize the depth as well. As it has been discussed in previous section, the whole laser ultrasonic wave forms can be transformed into a series of images. The consecutive images show how the different phases of the structure evolve in time. Fig. 10 show several selected frames from a series taken for a NASP heat exchanger sample with cooling channels. The scan area for these images is 6.0mm x 6.0mm. The "fingers" represent sharply the lower and the upper channels of the structure. It is of interest to compare the different phases of the upper channels and the lower ones shown in the images. If the recorded wave forms are long enough one can see the phases of the structures changing from negative (darker) to positive (brighter) or vice versa. Apparently the lower ones have a phase delay or a time lag when revealing the structure at different stages. The upper channels are actually closer to the surface. The time difference can be obtained, for example, from Fig. 10(b) and 10(c). Using the ultrasonic velocity, the difference of the depths between the upper and the lower channels can then be calculated.

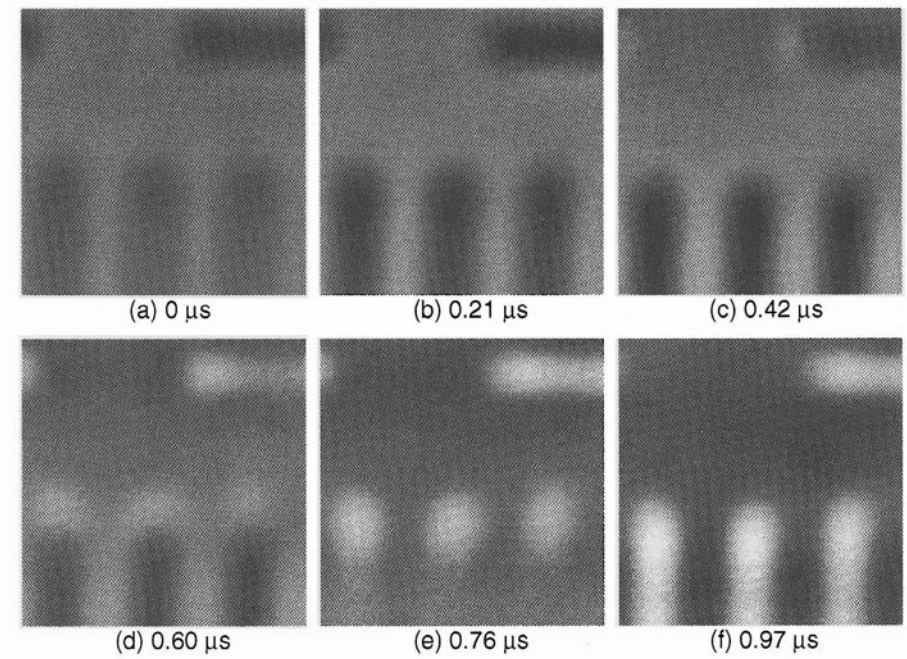

Fig. 10 A series of laser ultrasonic images of a NASP heat exchanger sample. The time for each frame is the relative change of the time-of-flight with respect to the first frame. Compared to the upper fingers, the lower ones have a phase lag. It indicates a difference of the depth below the surface.

CONCLUSION

Two techniques, laser ultrasonics and photoacoustics, are used for imaging in this research. They can be complementary to each other when used for the characterization of the subsurface structures. The photoacoustic magnitude images are more sensitive to surface treatments, as compared to the phase or laser ultrasonic images. Both the photoacoustic phase images and laser ultrasonic images can be a tool for the characterization of the depth for the subsurface structure. Coupling with the knowledge of the ultrasonic velocity, the laser ultrasonic technique seems to be more promising to obtain quantitative results.

ACKNOWLEDGEMENT

The authors want to thank Judith G. Moore of AS&M. Hampton, Virginia for her versatile computer program, which converts data into a movie format.

REFERENCES

1. A. Rosencwaig and A. Gersho, J. Appl. Phys. 47, 64 (1976).
2. D. A. Hutchins, in *Physical Acoustics*, Vol.XVIII, edited by W. P. Mason and R.N. Thurston (Academic Press, San Diego, 1988), Chap. 2.
3. F. A. McDonald and G. C. Wetsel, Jr., in *Physical Acoustics*, Vol.XVIII, edited by W. P. Mason and R.N. Thurston (Academic Press, San Diego, 1988), Chap. 4.
4. W. Jackson and N. M. Amer, J. Appl. Phys. 51, 3343 (1980).
5. G. Busse, in *Physical Acoustics*, Vol.XVIII, edited by W. P. Mason and R.N. Thurston (Academic Press, San Diego, 1988), Chap. 7.
6. C. B. Scruby and L. E. Drain, *Laser Ultrasonics: Techniques and Application*, (Adam Hilger, Bristol, 1990).
7. G. Busse and A. Rosencwaig, Appl. Phys. Lett. 36, 815 (1980).
8. D. A. Hutchins, F. Nadeau, P. Cielo, Can. J. Phys. 64, 1334 (1986).